# Correlation between Oligothiophene Thin Film Transistor Morphology and Vapor Responses

**L. Torsi,*,†,‡ A. J. Lovinger,† B. Crone,† T. Someya,† A. Dodabalapur,*,† H. E. Katz,*,† and A. Gelperin†**

*Bell Laboratories, Lucent Technologies, Murray Hill, New Jersey 07974, and Dipartimento di Chimica, Centro di Eccellenza T.I.R.E.S., Università degli Studi di Bari, 4 Via Orabona I-70126, Bari, Italy*

*Received: June 21, 2002; In Final Form: September 11, 2002*

Oligothiophene thin film transistors have recently been shown to respond to organic vapors, suggesting possible applicability in the field of olfactory sensor arrays. Here, we present a study of the correlation between the morphological structure of the active semiconductor thin film and the response to the vapor. The study was carried out by combining the measurement of the transient source−drain current of the transistor under vapor flow with the morphological characterization of the organic thin films by transmission electron microscopy.

## Introduction

Electronic olfaction is a very active research area being investigated by several research groups.[1] While progress in several sensor technologies has been encouraging, there is still need for a platform that possesses all of the required features of sensitivity, reliability, and reproducibility at low cost. Organic thin film transistors (OTFTs) are being investigated for use in low-cost flexible circuits[2,3] and displays.[4−7] We have already shown that organic transistors respond to a wide range of vapors.[8−10] Changes in several parameters can be observed as a result of exposure to chemical species.[8] Moreover, OTFTs employing different active layers have been demonstrated to respond to a large variety of vapors with good stability and significant sensitivity.[9] For example, 1-nonanol was tested with dialkylsexithiophenes and responses in the 5−10% range were measured for 10 ppm concentration. Gas-sensing complementary circuits and logic gates made from OTFTs have also recently been demonstrated.[11]

In this paper, we describe the influence of thin film molecular structure and morphology on the device response. We find that the morphology of the polycrystalline thin films plays an important role in determining the extent and nature of the response. The length of end groups and the size of the grains composing the thin films both affect the device responses. This study has been carried out with the combined use of electrical measurements of transient source−drain current under vapor flow and morphological characterization of the organic thin films by transmission electron microscopy (TEM).

## Experimental Section

The transistor structure employed for vapor sensing is shown in Figure 1a. Details of the fabrication and operation of similar devices have been reported elsewhere.[12] The substrate is a highly conducting silicon wafer coated with either 25 or 100 nm of silicon dioxide, thinner than typically used for OTFT demonstrations. The principal organic semiconductor is a thin film of α,ω-dihexyl-α-hexathiophene (DHα6T)[13,14] deposited by vacuum sublimation at $10^{-6}$ Torr over the silicon substrate. In one set of experiments, DHα6T thin films, of nominally the same thickness (70 nm average), were deposited for a range of substrate temperatures (measured directly over the $SiO_2$ layer) from room temperature to 170 ± 5 °C. A second series of DHα6T thin films, with average thicknesses from 27 to 70 nm, were deposited keeping the substrate nominally at room temperature. This procedure was adopted in order to investigate the dependence of the sensor response on the surface morphology, since the latter changes with the temperature of the substrate during deposition and with the thickness of the thin film. Transistors fabricated from different oligomers such as α-hexathiophene (α6T), α,ω-dibutyl-α6T (DBα6T), α,ω-didodecyl-α6T (DDDα6T), α,ω-dioctadecyl-α6T (DODα6T), and α,ω-dihexyl-α-quaterthiophene[15] were also evaluated.

Source (S) and drain (D) gold pads were thermally evaporated through a shadow mask with a spacing of $L = 200\ \mu$m directly over the organic film, while the gate (G) contact was defined by the silicon substrate. This device configuration allows the organic semiconductor to function simultaneously as both transistor channel material and vapor-sensing layer during exposure to the analyte atmosphere. A saturated vapor of 1-pentanol in a dry air carrier gas was typically used as the analyte, and saturated octanonitrile vapor was employed for comparison. The concentration of the vapors was in the thousand parts per million range.

The transistors were subjected to a constant flow rate of gas, which was switched between dry air and the vapor using the experimental apparatus described elsewhere.[9] The delivery system consisted of a peristaltic pump connected to sealed syringes containing either a saturated atmosphere of the target vapor or just the carrier gas. The alcohol and the octanonitrile (purchased from Aldrich, electronic grade) were used without further purification. It was previously shown[9] that responses were not due to water vapor. For the morphological characterization, organic thin films were deposited on carbon-coated electron microscope grids simultaneously with the TFT substrates. The films on the grids were obliquely shadowed with Pt/C to increase contrast and examined under bright field at 100 kV in a JEOL transmission electron microscope. The

† Lucent Technologies.
‡ Università degli Studi di Bari.

10.1021/jp021473q CCC: $22.00 
Published on Web 11/12/2002

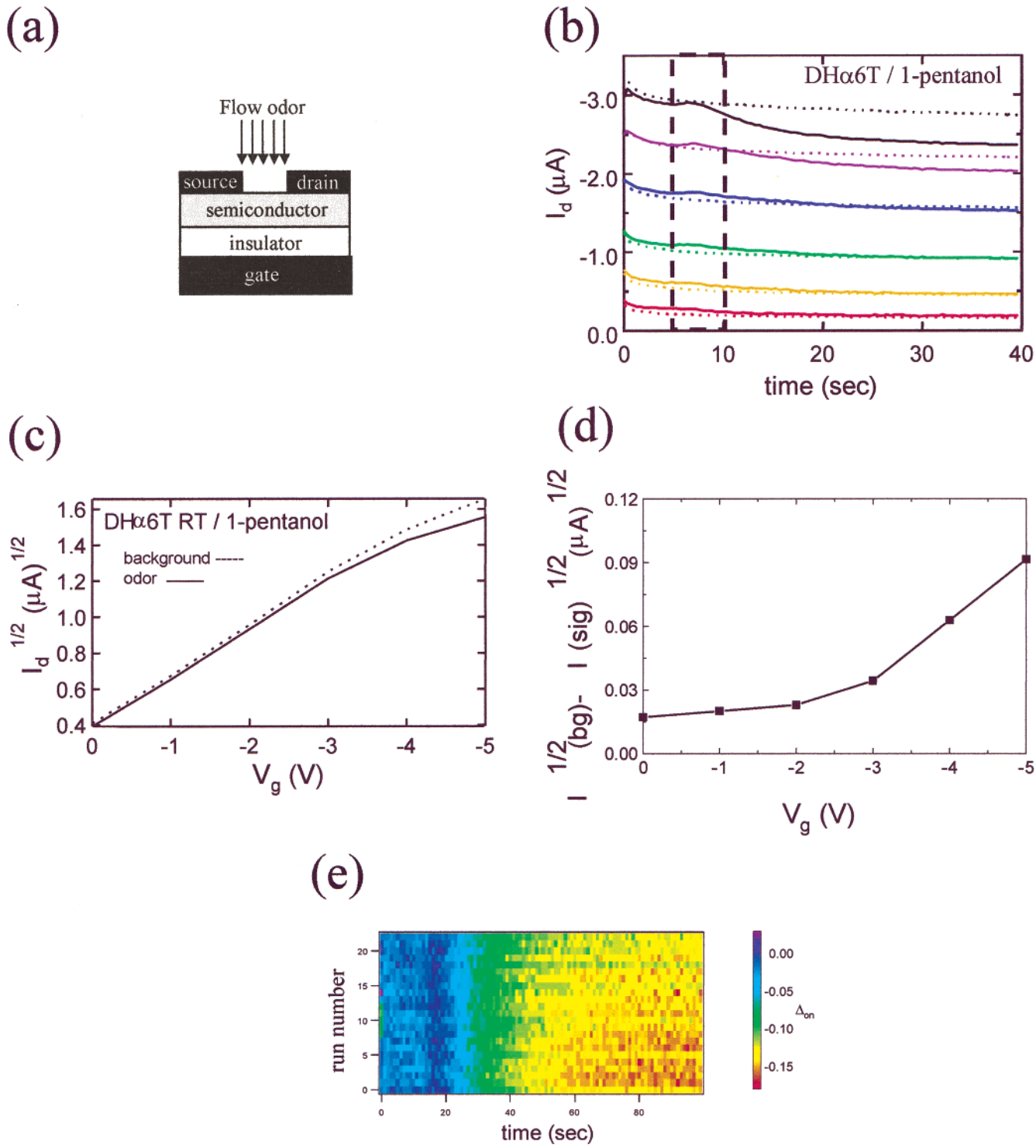


**Figure 1.** (a) Schematic of a OTFT sensor. An OTFT comprises a highly conductive Si wafer (resistivity 5−10 Ω cm) with a dielectric layer on top. The silicon substrate with a gold contact functions as the gate, and the top layer functions as the gate dielectric. An organic layer is then deposited on top of the dielectric by vacuum sublimation. The source and drain electrodes are gold pads with a spacing of $L = 200$ $\mu$m. (b) Saturated source−drain currents [at $V_g = 0$ V (red lines), −1 V (orange lines), −2 V (green lines), −3 V (blue lines), −4 V (violet lines), and −5 V (black lines)] of a DHα6T field effect sensor with and without exposure to 1-pentanol. The dotted lines are the background currents while the solid lines are the signals. The vapor molecules are delivered during the 5 s indicated by the dotted rectangle. (c) Square root of the saturated source−drain current as a function of gate voltage with and without exposure to 1-pentanol. (d) Difference of traces in panel c as a function of gate voltage. (e) Color-coded change in sensor current for 25 exposures of a DHα6T sensor (with a gate dielectric thickness of 25 nm) to 1-pentanol (see text for details).

correlation between mophologies of films grown on the two kinds of surfaces has been previously established.[16]

All of the semiconductors used as active layers in this study function as p-channel transistor materials. Therefore, the current−voltage (I−V) characteristics were measured in accumulation mode and in common source configuration,[17] applying negative source−drain ($V_{ds}$) and gate−source ($V_g$) biases both ranging between 0 and −5 V. For $V_{ds}$ equal to −5 V, the

transistors were in the saturated regime[12] even at the highest $V_g$ bias and the device intrinsic on/off ratios[14] ranged from 100 to 10 000.

Sensor responses were evaluated by measuring the transient saturated source−drain current ($I_d$) at a fixed $V_{ds}$ value ($V_{ds} = -5$ V). A simple expression for the saturated $I_d$ in a OTFT is given by

$$I_d = \frac{W \cdot C_i}{2 \cdot L} \cdot \mu_{FET} \cdot (V_g - V_T)^2 \quad (1)$$

where $V_T$ is the threshold voltage and $\mu_{FET}$ is the field effect mobility. $L$ and $W$ are the channel length and width, respectively, while $C_i$ is the $SiO_2$ capacitance per unit area.

## Results

Solid and dotted lines in Figure 1b are signal [$I_d$(sig)] and background [$I_d$(bg)] saturated source−drain currents vs time, measured with and without 1-pentanol introduced to the device, respectively. The vapor molecules are delivered during the 5 s indicated by the dotted rectangle. The plot in Figure 1c shows the square root of saturated $I_d$ values taken at 40 s as a function of gate bias. The difference between the two traces is plotted against gate voltage in Figure 1d. The decrease in the square root of the drain current upon vapor exposure is very small and relatively constant with respect to gate bias lower than 3 V, implying a negligible threshold shift with mobility remaining almost constant. At higher gate voltages, the "shift" is larger and no longer constant, implying a gate voltage-dependent mobility change.

The long-term stability of the OTFT sensors considered here can best be seen by considering the relative responses of the sensors, which were calculated using the following equation:

$$\Delta = \frac{|I_d(\text{sig}) - I_d(\text{bg})|}{I_d(\text{bg})} \quad (2)$$

The very good reproducibility of OTFTs employed as vapor sensors is documented by the results reported in Figure 1e, where the Δ-on of a DHα6T TFT sensor exposed to 1-pentanol is reported for 25 consecutive runs. During each run, the sensor was subjected to a duty cycle that comprises two steps during which the device is forward biased at $V_g = +3$ V for a few seconds with and without vapor flowing; between each of these steps, the sensor was subjected to a reverse bias in the absence of vapor. The reverse bias was introduced after having empirically observed that for primary alcohols, a reverse $V_g$ bias of +3 V affected a restoration of $I_d$ to near its original value. This behavior and the gate voltage-dependent mobility change described above are consistent with the pentanol binding electrostatically to the device in its "on" state.

The morphological dependence of OTFT responses to vapors has been studied as a function of the substrate deposition temperature for 70 nm thick DHα6T TFT sensors. In Figure 2 are shown transmission electron micrographs of samples grown at four different substrate temperatures. The morphology at room temperature and 70 °C (panels a and b) is seen to consist of very small, irregular nanodomains with diffuse grain boundaries, through which the vapors may penetrate the thin film and bind near the channel. Above that temperature, the granular morphology is replaced by a much more regular, lamellar one exhibiting much lower surface roughness (panels c and d). These grains are large, regular, and flat, thus reducing the ability of gases to adsorb onto them. The influence of the surface morphology of

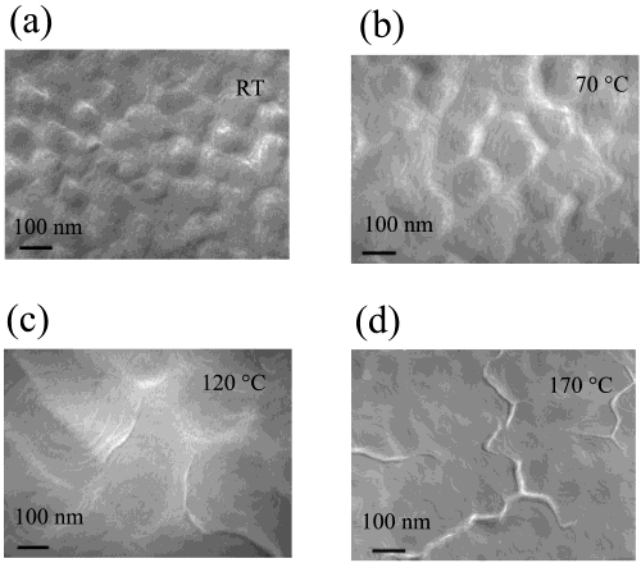


**Figure 2.** Transmission electron micrograph from a DHα6T film deposited by thermal evaporation keeping the substrate at (a) nominally room temperature, (b) $T = 70$ °C, (c) $T = 120$ °C, and (d) $T = 170$ °C.

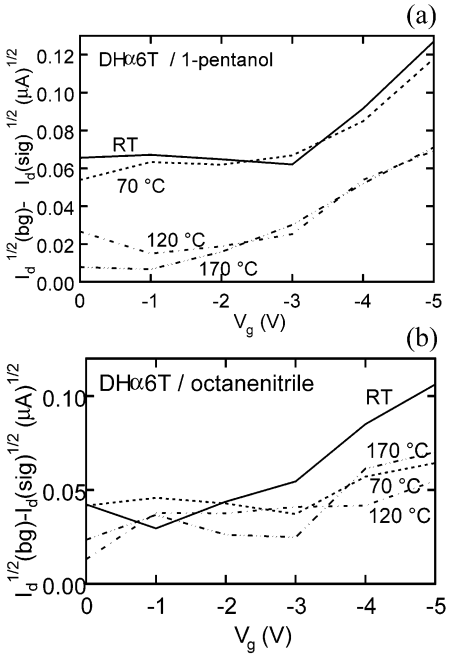


**Figure 3.** Change in square root of drain current as a function of gate voltage, for sensors with DHα6T films deposited at different substrate temperatures exposed to 1-pentanol (a) and to octanenitrile (b).

the various DHα6T films on the sensor response is illustrated in Figure 3, where the [$I_d$(sig)1/2 − $I_d$(bg)1/2] vs $V_g$ plots are reported for a OTFT sensor exposed to 1-pentanol (a) and octanenitrile (b). For 1-pentanol, two distinct regimes are evident, with the responses of samples grown at temperatures 70 °C or lower being more intense than those of samples grown at higher temperatures. The response is strong for the low-temperature films, which have more grain boundaries, and weaker for the high-temperature ones with fewer grain boundaries and a more compact morphology; this implies that for alcohols, the response of the sensor depends on interaction at grain boundaries. Note that the elevated teperature is capable of changing both the number and the electrical nature of the grain boundaries.

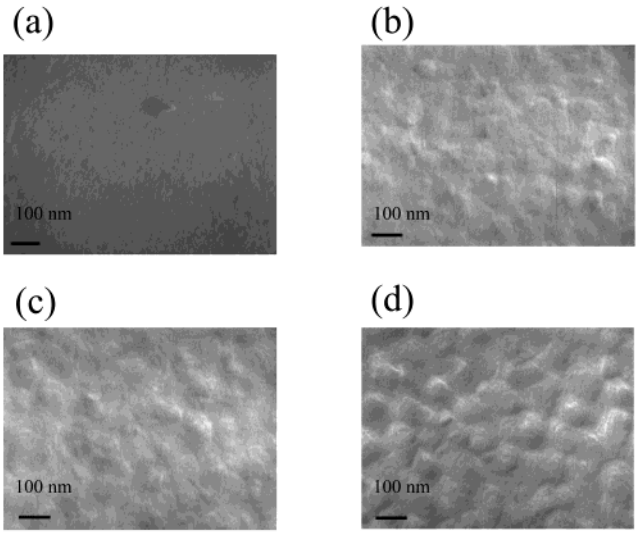


**Figure 4.** Transmission electron micrograph from a DHα6T film of different thicknesses (a, 27 nm; b, 53 nm; c, 61 nm; and d, 70 nm) deposited by thermal evaporation keeping the substrate nominally at room temperature.

On the other hand, the response to octanonitrile is independent of film morphology. This insensitivity to morphology in the response could be because the octanenitrile exerts its influence by a different mechanism or at a different binding site. For example, the highly dipolar nitrile functional group might be capable of creating an effective hole trap even while adsorbing to the top surface of the film, rather than at a grain boundary. We cannot rule out the possibility that octanonitrile could attack the contacts and limit injection. The important observation is that the set of devices responds in different ways to different vapors, providing a means of creating a diverse array of sensing elements for olfactory discrimination.

The correlation between the morphology of films with different thicknesses and the relevant responses has been investigated. In particular, the morphological appearance of a film 27 nm thick is studied in order to get insights on a region where charge is confined in a FET device. The charge accumulation layer is in fact much thinner (few nm thick),[17] but the study of such a thin film, particularly as part of a sensing device, could not be accomplished because the coverage of the channel region was often incomplete. The morphology of DHα6T films of different thicknesses deposited at room temperature is shown in Figure 4. The surface of the ultrathin film (panel a) appears flat and almost featureless, and only few regions are covered by three-dimensional grains. The surface morphology becomes more structured as the films grow thicker (panels b−d); slightly elongated grains, which can be as large as ca. 50−100 nm, cover larger areas becoming clearly contiguous in the thicker specimen. An increase in their height occurs as well. As a result, the number of grains in the films as well as of grain boundaries increases with DHα6T film thickness. The influence of the surface morphology of DHα6T film of different thickness on the device response is illustrated in Figure 5, where plots of $[I_d(\mathrm{sig})1/2 - I_d(\mathrm{bg})1/2]$ vs $V_g$ are reported for a TFT exposed to 1-pentanol. The response increases with increasing film thickness because an increase in the thickness of the deposited film also increases the number of grains and grain boundaries, providing more sites of interaction with the vapor. Even though these sites may be farther from the dielectric interface than the two monolayer extent of the channel, they could still trap charge from the

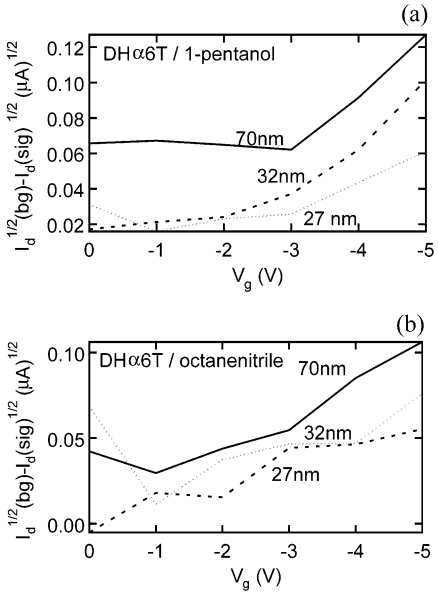


**Figure 5.** Change in square root of drain current as a function of gate voltage, for sensors with DHα6T films of different thicknesses exposed to 1-pentanol (a) and to octanenitrile (b).

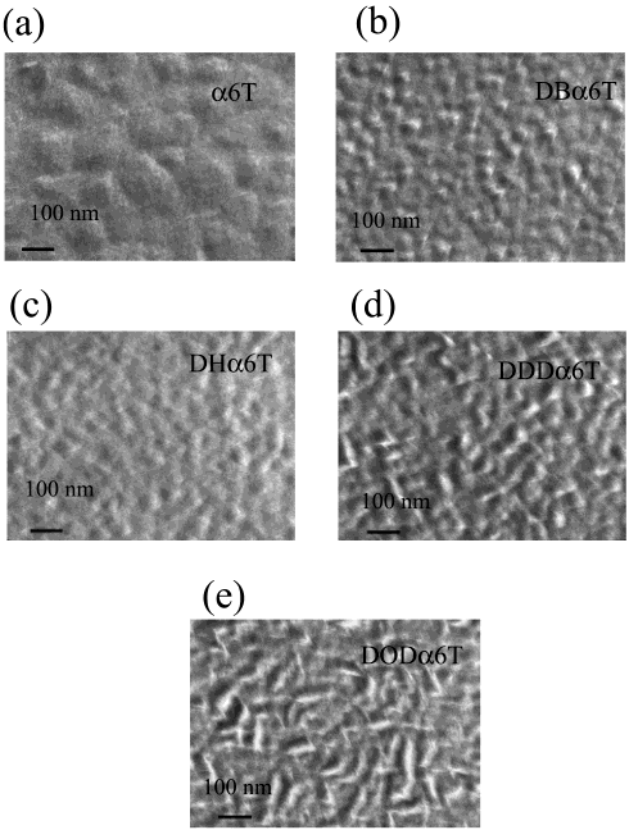


**Figure 6.** Transmission electron micrograph from α6T (a), DBα6T (b), DHα6T (c), DDDα6T (d), and DODα6T (e) films (70 nm thick) deposited by thermal evaporation keeping the substrate nominally at room temperature.

channel. For comparison, Figure 5b shows a similar plot for octanenitrile, which is less conclusive.

We have also examined the morphology of a series of alkyl-substituted hexathiophenes homologues. Thin films were deposited on a substrate held at room temperature; their surface morphology can be seen in Figure 6. The parent material, α-6T, is seen to have a compact structure consisting of ca. 100 nm

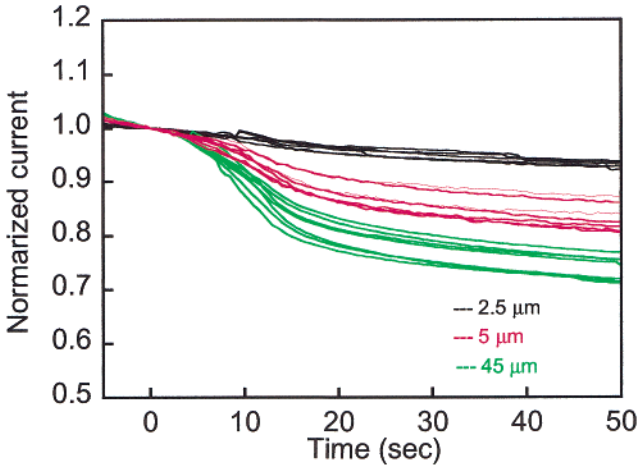


**Figure 7.** Response of DHα4T devices of different lengths to pentanol vapor. The semiconductor film was grown on a 70° substrate.

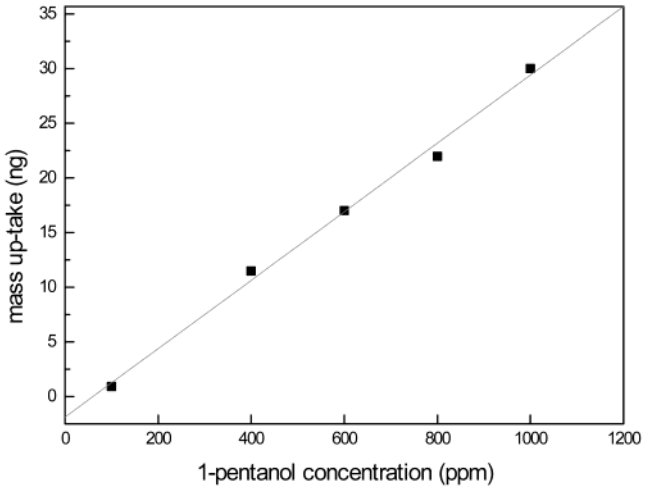


**Figure 8.** Mass uptake by a polycrystalline DHα4T film as a function of pentanol concentration in the ambient atmosphere.

sized grains. The dibutyl- and dihexyl-substituted 6T exhibit much smaller grains, for which therefore the high degree of surfaces roughness and grain boundaries constitute a proportionately larger fraction of the material, thus promoting binding of vapors. Didodecyl 6T begins to show some elongation of these grains, which tend toward lamellar morphology and which thus are packed more loosely allowing greater access of vapors. This elongated lamellar morphology becomes fully apparent for dioctodecyl 6T, as does their much looser mutual packing (Figure 6e). This trend is consistent with the increased responses of alkyl-containing 6Ts to primary alcohol vapors. Evidence has already been provided in the literature[9] that vapor responses of alkyl-substituted hexathiophene TFTs increase as the length of the 6T hydrocarbon end group increases. Such behavior has been observed for 1-alcohols as well as for other molecules. The larger alkyl substituents on the oligomers could enhance the device response by increasing the adsorptivity of grain surfaces, by increasing the amount and the accessiblity grain surface area, and by changing the electronic or spacial barriers between grains.

Finally, we investigated the behavior of a shorter oligomer, α,ω-dihexyl-α-quaterthiophene. Films of this compound grown on room temperature substrates have submicrometer granular morphologies similar to those shown in Figure 6b,c and are considerably sensitive to pentanol exposure, as shown in Figure 7. When such films are deposited on a quartz crystal and exposed to controlled concentrations of pentanol delivered via computer-controlled flow-meters, the mass uptake, evaluated with an in-flow microbalance system, is linear ($R = 0.997$) in the 100−1000 ppm range, as shown in Figure 8. This is an important result since it ties the dose−response relationship to mass uptake, at least in the limited range investigated. The rate of unassisted reversibility of the mass response was very poor; the time scale for restoring the baseline value was about 1 h. This behavior illustrates the value of the gate reverse bias in promoting the reset of the sensing device in the experiment of Figure 1e.

The degree of pentanol-induced swelling of the same thin films was evaluated by means of a single wavelength (632.8 nm) ellipsometer. Many high molecular weight polymers undergo swelling phenomena when exposed to organic vapors.[18] The swelling process is very similar to a conventional dissolution process as it depends on the hydrophilic or hydrophobic character of the solvent/polymer binary system. During the exposure of the DHα4T film to 100 ppm pentanol vapors, the film refractive index remained constant and identical to the preexposure value ($n = 1.361$ and $k = 0$). Neither was any thickness variation of the film observed. These results imply that the interaction between the alcohol and the DHα4T film does not involve the bulk of the film; most reasonable is a surface type interaction involving gain boundaries.

DHα4T deposited on a 70 °C substrate exhibits a nearly single-crystal morphology over 10 μm or more.[15] Devices made in the typical way from this larger grain film were also sensitive to pentanol, but extremely short channel length devices, with ca. 2 μm S−D distance, were completely insensitive to pentanol, since no grain boundaries were traversed by the channels of those devices. The behavior of this material is discussed in greater depth in a separate communication.[19]

In conclusion, TEM and electrical measurements of variously alkyl-substituted thiophene oligomer transistors under pentanol vapor have demonstrated that the response is enhanced as the number of grain boundaries increases. The morphological and electrical evidence is consistent with the interaction of alkyl-substituted oligothiophene thin films with alcohols occurring most probably at the grain boundaries with the alkyl chains facilitating the adsorption of the vapor molecules by the sensing film. The means by which this adsorption occurs are probably a combination of favorable hydrophobic interactions between the semiconductor and the alcohol alkyl chains, intercalation to fill defect vacancies in the hydrocarbon layers of the film, and simple surface binding. All of these would be favored at grain boundaries. These tend to be rougher than top surfaces of grains, so there are more molecular scale channels for incorporation of analyte. The lattice direction mismatch between pairs of grains that abut each other inevitably adds to the disorder and free volume of layers near the boundary. Finally, semiconductor film thickness is less near grain boundaries, as observed by TEM, so analytes binding there would be closer to the channel and thereby exert greater influence on electrical responses.

On the other hand, a different mechanism, less tied to the alkyl chains, seems to be operative for octanenitrile, as well as for the previously studied interaction of unsubstituted α-6T with 2-heptanone.[9] It is important to note that comparable insights would be hard to obtain if a resistor was used instead of a thin film transistor as the sensing device. A resistor is sensitive to bulk mobility changes, whereas a transistor is sensitive not only to changes in the channel mobility but also to the number of trapped or otherwise immobile charges, which give rise to a threshold shift. The design of binding sites, whether physical

clefts or specific molecular subunits, to capture analytes should lead to more sensitive and selective detection.

**Acknowledgment.** We are indebted to Dr. I. Farella for performing swelling experiments and A. Tafuri for performing quartz crystal microbalance measurements.

## References and Notes

(1) Gardner, J. W.; Bartlett, P. N. *Electronic Noses*: *Principles and Applications*; Oxford University Press: Oxford, 1999.

(2) Bao, Z.; Feng, Y.; Dodabalapur, A.; Raju, V. R.; Lovinger, A. J. *Chem. Mater*. **1997**, *9*, 1299.

(3) Drury, C. J.; Mutsaers, C. M. J.; Hart, C. M.; Matters, M.; de Leeuw, D. M.; et. al. *Appl. Phys. Lett*. **1999**, *73*, 108.

(4) Sirringhaus, H.; Tessler, N.; Friend, R. H. *Science* **1998**, *280*, 1741.

(5) Dodabalapur, A.; Bao, Z.; Makhija, A.; Laquindanum, J. G.; Raju, V. R.; Feng, Y.; Katz, H. E.; Rogers, J. *Appl. Phys. Lett*. **1998**, *73*, 142.

(6) Jackson, T. N.; et al. *IEEE J. Sel. Top. Quantum Electron. 4* **1998**, 100.

(7) Blanchet, G. Presented at the Spring 2002 meeting of the American Chemical Society.

(8) Torsi, L.; Dodabalapur, A.; Sabbatini, L.; Zambonin, P. G. *Sens. Actuators, B* **2000**, *67*, 312.

(9) Crone, A.; Dodabalapur, A.; Gelperin, A.; Torsi, L.; Katz, H. E.; Lovinger, A. J.; Bao, Z. *Appl. Phys. Lett*. **2001**, *78*, 2229−2231.

(10) Torsi, L.; Dodabalapur, A.; Cioffi, N.; Sabbatini, L.; Zambonin, P. G. *Sens. Actuators, B* **2001**, *77* (1−2), 7−11.

(11) Crone, B.; Dodabalapur, A.; Sarpeshkar, R.; Gelperin, A.; Katz, H. E.; Bao, Z. *J. Appl. Phys*. **2002**, *91*, 10140.

(12) Torsi, L.; Dodabalapur, A.; Katz, H. E. *Appl. Phys. Lett*. **1995**, *78*, 1088.

(13) Katz, H. E.; Laquindanum, J. G.; Lovinger, A. J. *Chem. Mater*. **1998**, *10*, 633.

(14) Garnier, F.; Yassar, A.; Hajlaoui, R.; Horowitz, G.; Deloffre, F.; Servet, B.; Ries, S.; Alnot, P. *J. Am. Chem. Soc*. **1993**, *115*, 8716.

(15) Katz, H. E.; Lovinger, A. J.; Laquindanum, J. G. *Chem. Mater*. **1998**, *10*, 457.

(16) Lovinger, A. J.; Davis, D. D.; Ruel, R.; Torsi, L.; Dodabalapur, A.; Katz, H. E. *J. Mater. Res*. **1995**, *10*, 2958.

(17) Dodabalapur, A.; Torsi, L.; Katz, H. E. *Science* **1995**, *268*, 270.

(18) Lonergan, M. C.; Severin, E. J.; Doleman, B. J.; Beaber, S. A.; Grubbs, R. H.; Lewis, N. S. *Chem. Mater*. **1996**, *8*, 2298.

(19) Someya, T.; Katz, H. E.; Gelperin, A.; Lovinger, A. J.; Dodabalapur, A. *Appl. Phys. Lett*. **2002**, *81*, 3079.

(20) Torsi, A.; Dodabalapur, A.; Katz, H. E.; Lovinger, A. J.; Ruel, R. *MRS Symp. Proc*. **1995**, *37*, 695.